

Bayesian Approach to Segmentation of Statistical Parametric Maps

Jagath C. Rajapakse*, *Senior Member*, and Jayasanka Piyaratna, *Student Member*

Abstract—A contextual segmentation technique to detect brain activation from functional brain images is presented in the Bayesian framework. Unlike earlier similar approaches [Holmes and Ford (1993) and Descombes *et al.* (1998)], a Markov random field (MRF) is used to represent configurations of activated brain voxels, and likelihoods given by statistical parametric maps (SPM's) are directly used to find the maximum a posteriori (MAP) estimation of segmentation. The iterative segmentation algorithm, which is based on a simulated annealing scheme, is fully data-driven and capable of analyzing experiments involving multiple-input stimuli. Simulation results and comparisons with the simple thresholding and the statistical parametric mapping (SPM) approaches are presented with synthetic images, and functional MR images acquired in memory retrieval and event-related working memory tasks. The experiments show that an MRF is a valid representation of the activation patterns obtained in functional brain images, and the present technique renders a superior segmentation scheme to the context-free approach and the SPM approach.

Index Terms—Bayesian methods, fMRI, functional brain imaging, Gaussian random fields, Markov random fields, MAP estimation, statistical parametric mapping.

I. INTRODUCTION

FUNCTIONAL magnetic resonance imaging (fMRI) and positron emission tomography (PET) are popular modalities to image the working human brain [4], [5]. Functional brain studies acquire a series of head scans while the subject is alternately performing a major sensory or cognitive task and a baseline task [6], where the input stimulus to the brain takes the form of an ON-OFF box-car pattern. The first step in the analysis of functional brain images is to detect brain regions that are activated by input stimuli [5]. This may be seen as a classification or segmentation of brain voxels into activated voxels and inactive voxels during a functional experiment.

The detection of brain activation due to an input stimulus is performed by statistically comparing images taken during stimulation (ON state) and those taken when the brain is at rest (OFF state). The results of comparisons are expressed by generating test statistics for every brain voxel, where each statistic indicates the likelihood or the significance of activation of the corresponding voxel by that stimulus. Such statistics, obtained over

all brain voxels, form *statistical parametric maps* (SPMs) of the brain.

An SPM is an image in which intensity values represent statistics obtained under the null hypothesis of no activation and conform to a certain probability distribution. Thresholding an SPM at a proper significance value or p -value can detect significant brain activation. However, such an approach does not provide correction for multiple statistical comparisons or spatial correlation present in SPMs [7]. The theory of Gaussian random fields (GRFs) has been utilized to incorporate the spatial correlation into the thresholding scheme [8], in which intensity values of the SPMs are considered to be a random field where the joint density of any subset of the field is given by a multivariate Gaussian distribution. This approach is referred to as *statistical parametric mapping* (SPM) [9]. The GRF theory allows the computation of corrected p -values that compensate for the clusters of false positives over the entire brain volume, and relates the significances of activation to the spatial extents of the activated blobs [7], [8].

The GRF assumption requires spatial filtering of functional images in order to avoid voxels that, due to the random nature of the field, appear to be activated [3], [10], and enhances the significance of statistics in the activated regions by taking into account their spatial extent. This process increases the significances of activated regions with large extent and lowers the significances of small regions of activation. So the SPM approach may be less sensitive to strongly active regions with small extent and may misinterpret large regions having small significances. The results of the GRF theory are also exact only at high threshold values of statistics [11]. Furthermore, filtering functional images to ensure that they conform to the GRF theory may suppress significant high-frequency spatial information [2], [3].

In this paper, we present an alternative approach to process SPMs, assuming that the activation patterns form Markov random fields (MRFs) [12]–[15]. In the past, a complex spatio-temporal MRF has been used to restore signals and to represent intensity distributions of SPMs [1]–[3], and Bayesian modeling of fMRI time-series to infer hidden psychological states in fMRI experiments was considered in [16]. Our aim is to detect significant brain activation by presuming that the activation patterns of brain voxels form binary MRFs and using the likelihoods of the activation directly obtained from the SPMs. In short, we show how the posterior probabilities can be derived from likelihoods given by intensities of the SPM and the prior probabilities given by clique potentials, reflecting the fact that the underlying spatial pattern of activation should conform to a biologically plausible MRF. Our approach harnesses the spatial structure of the data to turn a likelihood-based approach into a

Manuscript received September 4, 2000; revised June 24, 2001. This work was supported in part by grants from the National Science Foundation (NSF). Asterisk indicates corresponding author.

*J. C. Rajapakse is with the School of Computer Engineering, Nanyang Technological University, Block N4, Nanyang Avenue, Singapore 639798, Singapore (e-mail: asjagath@ntu.edu.sg).

J. Piyaratna was with the School of Computer Engineering, Nanyang Technological University, Singapore 639798, Singapore.

Publisher Item Identifier S 0018-9294(01)08284-2.

Bayesian approach [17] that explicitly accommodates the local spatial smoothness of activation profiles. An iterative algorithm based on a simulated annealing (SA) technique [18] finds the maximum *a posteriori* (MAP) probability estimation [14], [15] of brain activation and provides a complete data-driven scheme for segmentation of SPMs.

The paper is organized as follows. Section II describes the SPM approach, the MRF model for brain activation pattern and how the MAP estimation is derived. The iterative segmentation algorithm is described in Section III, and the results of segmentation of synthetic functional images and functional MR data obtained in memory retrieval and event-related working memory experiments are presented in Section IV. The results are compared with the simple thresholding and the SPM techniques, and finally the conclusions are made.

II. THEORY

A functional brain image is a spatio-temporal signal consisting of a series of brain scans taken over time. Let $F: \Omega \times \Theta \rightarrow \mathcal{Q}$ be a functional image, where $\Omega \subset \mathbf{N}^3$ denotes the three-dimensional spatial domain of image voxels, Θ the space of scanning times and $\mathcal{Q} \subset \mathbf{R}$ the range of image intensity. As head scans are acquired at regular intervals of time, one may write $\Theta = \{\Delta, 2\Delta \cdots n\Delta\}$ where Δ denotes the scanning interval and n the total number of image scans. By an *image scan*, we mean an image of the subject's head, or a part of it, taken at a particular instance of time; and by a functional *time-series*, we mean a restriction to the functional image at a particular voxel.

Before the analysis of functional images for detection of brain activation, preprocessing of the images is necessary. The set of brain voxels is first identified from the image domain, and the brain scans are corrected for baseline intensity variation and subject's head motion. Derivation of SPMs is usually the first step in the statistical analysis of functional images, in order to detect regions of significant activation. In what follows the analysis of SPMs is presented in the framework of the general linear model (GLM) [6], [19]. We let $\Omega_B \subset \Omega$ denote the set of brain voxels.

A. General Linear Model (GLM)

Consider an fMRI experiment involving multiple-input stimuli, and let $y(t)$ and $x_k(t)$ denote the values of the fMRI time-series response and the input stimulus k at time t , respectively. Let $\mathbf{x}_k = (x_k(t): t \in \Theta)^T$ and the *design matrix* of the experiment be $[\mathbf{x}_1 \ \mathbf{x}_2 \ \cdots \ \mathbf{x}_u \ \mathbf{x}_{u+1} \ \cdots \ \mathbf{x}_{u+v}]$ where $\mathbf{x}_1, \mathbf{x}_2 \cdots \mathbf{x}_u$ represent u stimulus covariates and $\mathbf{x}_{u+1}, \mathbf{x}_{u+2}, \cdots \mathbf{x}_{u+v}$ represent v dummy covariates (e.g., age, sex, etc.) [6], [10]. If $\mathbf{y} = (y(t): t \in \Theta)^T$ denotes the fMRI time-series, the GLM [6], [19] can be written as

$$\mathbf{y} = \mathbf{X}\boldsymbol{\beta} + \boldsymbol{\eta} \quad (1)$$

where $\boldsymbol{\beta} = (\beta_1, \beta_2, \dots, \beta_{u+v})^T$ denotes the regression coefficients relating the input covariates to the fMRI response, the matrix $\mathbf{X} = [\mathbf{H}_1\mathbf{x}_1 \ \mathbf{H}_2\mathbf{x}_2 \ \cdots \ \mathbf{H}_u\mathbf{x}_u \ \mathbf{x}_{u+1} \ \cdots \ \mathbf{x}_{u+v}]$ represents the design matrix having covariates modified with the *modulation matrices* $\mathbf{H}_k = \{h_{ij}^k\}_{n \times n}$, and the components of

the noise vector $\boldsymbol{\eta}$ are uncorrelated and normally distributed. In the case of gamma hemodynamic response function (HRF) [20]

$$h_{ij}^k = \frac{((i-j)/\tau_k)^{n_k-1} e^{-(i-j)/\tau_k}}{\tau_k \Gamma(n_k)} \quad (2)$$

where $\tau_k, n_k \in \mathbf{R}^+$ denote the parameters that relate to the lag and dispersion of the HRF of the stimulus k , and $\Gamma(\cdot)$ denotes the gamma function. The multiplication of an input stimulus with the corresponding modulating matrix takes into account the lag and the autocorrelation (i.e., dispersion) present in the fMRI response [6].

The following F statistic measures the significance of the stimulus $k \leq u$, producing the time-series \mathbf{y} [21]

$$F_k = d_k \frac{(\hat{\boldsymbol{\beta}}^T \mathbf{X}^T \mathbf{y} - \hat{\boldsymbol{\beta}}_k^T \mathbf{X}_k^T \mathbf{y})}{(\mathbf{y}^T \mathbf{y} - \hat{\boldsymbol{\beta}}^T \mathbf{X}^T \mathbf{y})} \quad (3)$$

where \mathbf{X}_k is given by $[\mathbf{H}_1\mathbf{x}_1 \ \cdots \ \mathbf{H}_{k-1}\mathbf{x}_{k-1} \ \mathbf{H}_{k+1}\mathbf{x}_{k+1} \ \cdots \ \mathbf{H}_u\mathbf{x}_u \ \mathbf{x}_{u+1} \ \cdots \ \mathbf{x}_{u+v}]$, the degrees of freedom $d_k = n - p - q - 1$, and $\hat{\boldsymbol{\beta}}_k$ is the coefficient vector $\boldsymbol{\beta}$ without β_k , that corresponds to \mathbf{X}_k . The least-square estimate of the regression coefficients $\boldsymbol{\beta}$ is given by $\hat{\boldsymbol{\beta}} = (\mathbf{X}^T \mathbf{X})^{-1} \mathbf{X}^T \mathbf{y}$.

B. Statistical Parametric Mapping (SPM)

By following (3) for each time-series at voxel site $p \in \Omega_B$ and stimulus condition \mathbf{x}_k , an F statistical score indicating the significance of predicting the time-series at voxel site p , $F_k(p)$ may be computed. The set $\mathbf{F}_k = \{F_k(p): p \in \Omega_B\}$ represents an F statistical map for the stimulus k and is denoted by $\text{SPM}\{F_k\}$ [6], [8]. SPMs obtained using one statistic can be converted to another statistic using their cumulative distributions [8]; for instance, z statistical SPM $\{z_k\}$ may be derived from $\text{SPM}\{F_k\}$.

Defining a threshold for an SPM to detect activation at a given significance level or p -value is not straightforward because corrections for multiple dependent statistical comparisons and adjustments for spatial correlations in the activation patterns need to be made [22]. The minimum size of the regions of significant activations above a given threshold on $\text{SPM}\{z\}$ s has been related to using the theory of GRFs [7], [8], [23], in which the regional excursions of SPMs are interpreted as regionally specific events or significant brain activations. The number of significant clusters or connected components above a certain threshold of intensity has been derived using the theory of zero crossings [22] and differential topology [24] and forms a Poisson distribution. The application of these results leads to significance values that indicate the spatial extents of the activated blobs. This approach requires that the intensity profile of the SPM is smooth and (usually) filtered before the analysis [3], [22].

C. Markov Random Field (MRF) Approach

The present approach presumes that the brain activation patterns form MRFs [12], [14] to incorporate contextual information. Let the set $\mathbf{a}_k = \{a_k(p) | p \in \Omega_B\}$ denote a segmentation of an SPM (or a configuration of brain activation, where $a_k(p)$ denotes the state of the brain voxel at site p and $a_k(p) = 0$ if the voxel is inactive and $a_k(p) = 1$ if the voxel is activated by

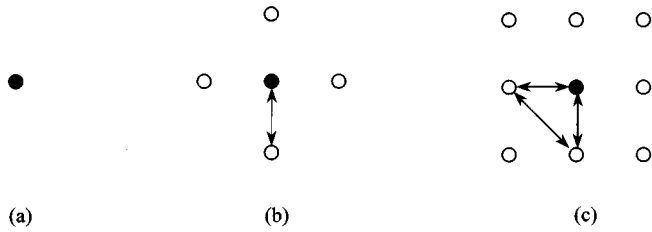


Fig. 1. Illustration of cliques at a pixel of an image: (a) singleton, (b) doubleton, and (c) tripleton cliques.

the stimulus k . If \mathbf{a}_k is an instance of an MRF, the Markovian property states [14] that

$$P(a_k(p)|a_k(q), q \neq p, q \in \Omega_B) = P(a_k(p)|a_k(q), q \in N_r(p)) \quad (4)$$

where $N_r(p) = \{q: \|p - q\|^2 \leq r^2, q \neq p, q \in \Omega_B\}$ is the r -order neighborhood of the voxel site p . Furthermore, according to the Hammersley–Clifford theorem, \mathbf{a}_k has a Gibbs distribution [12]

$$P(\mathbf{a}_k) = \frac{1}{Z} \exp\{-U(\mathbf{a}_k)\} \quad (5)$$

where the term $U(\mathbf{a}_k)$ represents a global energy of the configuration \mathbf{a}_k , and Z is the normalization factor. The temperature parameter often associated with the exponential term of (5) has been incorporated into the energy term. The energy $U(\mathbf{a}_k)$ is given by the sum of the potentials of the cliques of voxels in the image [14]

$$U(\mathbf{a}_k) = \sum_{c \in C} V_c(\mathbf{a}_k) \quad (6)$$

where C denotes the set of all cliques, and $V_c(\mathbf{a}_k)$ denotes the potential of the clique c , given the activation pattern \mathbf{a}_k . A *clique* is a subset of voxel sites, such that every pair of distinct sites in the subset are neighbors (see Fig. 1), and the potentials measure the spatial dependencies of the voxels in the cliques [14].

The energy $U(\mathbf{a}_k)$ can be written as a sum of the local energies over the voxel sites [14], [15]

$$U(\mathbf{a}_k) \propto \sum_{p \in \Omega_B} U_p(\mathbf{a}_k) \quad (7)$$

where $U_p(\mathbf{a}_k)$ denotes the *local energy* of the configuration \mathbf{a}_k at site p and can be written as

$$U_p(\mathbf{a}_k) = \sum_{p \in c: c \in C} V_c(\mathbf{a}_k). \quad (8)$$

As the state of a brain voxel is either activated or inactive, the MRF is assumed here to be a *binary logistic* model [25] in which a parameter β_l is associated with the potential for each clique type c_l irrespective of its constituents except at singleton cliques. For simplicity, if we restrict ourselves to the singleton and doubleton cliques of voxels in the image and up to the

second-order neighborhoods, the local energy can be written as [15], [25]

$$U_p(\mathbf{a}_k) = \alpha_{k0} \delta(a_k(p) = 0) + \alpha_{k1} \delta(a_k(p) = 1) - \sum_{\substack{p, q \in c: c \in C_1 \\ q \in N_1(p)}} \beta_{k1} \delta(a_k(p) = a_k(q)) - \sum_{\substack{p, q \in c: c \in C_2 \\ q \in N_2(p) \setminus N_1(p)}} \beta_{k2} \delta(a_k(p) = a_k(q)) \quad (9)$$

where

$\delta(\cdot)$	+1 if the condition inside is satisfied and -1 otherwise;
C_1 and $C_2 \subset C$	sets of all first-order and second-order doubleton cliques over Ω_B , respectively;
α_{k0} and $\alpha_{k1} \in \mathbf{R}^+$	potentials of singleton cliques when the voxel in consideration is inactive or active, respectively;
β_{k1} and $\beta_{k2} \in \mathbf{R}^+$	first-order and second-order doubleton clique potentials of activation by the stimulus k , respectively.

D. Maximum A Posterior (MAP) Criteria

Let the set $\mathbf{s}_k = \{s_k(p)|p \in \Omega_B\}$ represent an SPM $\{s_k\}$. The likelihood of an SPM, knowing the activity configuration, is given by the distribution of the underlying SPM, and (5) provides the prior probability of an activity configuration. Therefore the posterior probability $P(\mathbf{a}_k|\mathbf{s}_k)$ of the activation pattern \mathbf{a}_k , given the SPM \mathbf{s}_k , can be evaluated using the Bayes' theorem [17]

$$P(\mathbf{a}_k|\mathbf{s}_k) = P(\mathbf{s}_k|\mathbf{a}_k)P(\mathbf{a}_k) \quad (10)$$

where $P(\mathbf{s}_k|\mathbf{a}_k)$ indicates the likelihood of the SPM $\{s_k\}$.

Because the statistics of SPMs are evaluated independently, considering the time-series at each voxel site, $P(\mathbf{s}_k|\mathbf{a}_k) = \prod_{p \in \Omega_B} P(s_k(p)|a_k(p))$. Substituting this in (10), from (5), (7), and (8), the posterior probability $P(\mathbf{a}_k|\mathbf{s}_k)$ is given by

$$P(\mathbf{a}_k|\mathbf{s}_k) \propto \frac{1}{Z} \exp\{-V(\mathbf{a}_k)\} \quad (11)$$

where the posterior energy, $V(\mathbf{a}_k) = \sum_{p \in \Omega} \{U_p(\mathbf{a}_k) - \ln(P(s_k(p)|a_k(p)))\}$; the activity configuration \mathbf{a}_k^* rendering the MAP estimation [15] is given by

$$\mathbf{a}_k^* = \arg \min_{\mathbf{a}_k \in \mathcal{A}} V(\mathbf{a}_k) \quad (12)$$

where \mathcal{A} denotes the space of all activation configurations of brain voxels.

To minimize the posterior energy, we use a SA algorithm. The algorithm is iterative and considers the conditional probabilities on each site. The main characteristic of the SA algorithm is to accept increase of energy function randomly to escape from the local energy minima. The increase of energy accepted depends on a parameter, temperature T , which is initially set to a high value and gradually lowered to approach zero. Sampling from the distribution is done

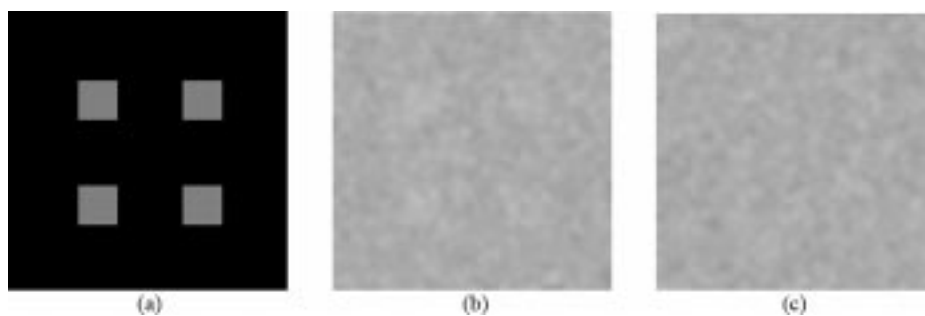


Fig. 2. The simulated functional image having a S/N ratio of -8.5 dB and a Gaussian spatial correlation of FWHM = 3.0 pixels. (a) Activated regions, (b) sixth image scan, and (c) tenth image scan.

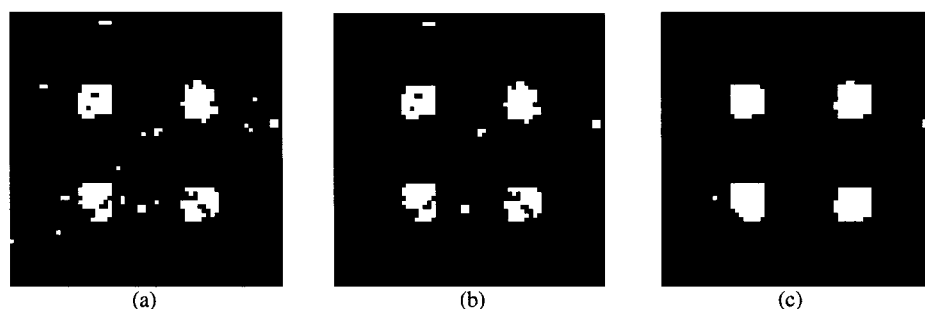


Fig. 3. Detected activation of the synthetic functional image by (a) thresholding the SPM $\{z\}$ at a significance of $p = 0.01$, (b) using the SPM approach on the SPM $\{z\}$ with a minimum blob size of three pixels and a significance threshold $z = 2.75$, and (c) using the MRF approach on the SPM $\{z\}$. The intensity values of the activated pixels correspond to the significances of activation.

proportional to $\exp\{-V(\mathbf{a}_k)/T\}$ using the Metropolis algorithm [26] in which the change of the local activation status, say $a_k^{\text{old}}(p)$, to the new status, say $a_k^{\text{new}}(p)$, is done with a probability given by $\min(\exp\{-V(\mathbf{a}_k: a_k(p) = a_k^{\text{new}}(p)) - V(\mathbf{a}_k: a_k(p) = a_k^{\text{old}}(p))\}/T, 1)$. That is, the present value of activation $a_k(p)$ is changed to a new value as follows:

```

if  $V(\mathbf{a}_k: a_k(p) = a_k^{\text{old}}(p)) > V(\mathbf{a}_k: a_k(p) = a_k^{\text{new}}(p))$ 
     $a_k(p) = a_k^{\text{new}}(p);$ 
else
    generate a random number  $\rho \in [0, 1]$ 
    if  $\rho < \exp\{-V(\mathbf{a}_k: a_k(p) = a_k^{\text{new}}(p)) - V(\mathbf{a}_k: a_k(p) = a_k^{\text{old}}(p))\}/T$ 
         $a_k(p) = a_k^{\text{new}}(p);$ 

```

III. SEGMENTATION ALGORITHM

An iterative algorithm is proposed to incorporate the present model to a segmentation scheme suboptimally and yield the MAP estimation of the activity configuration. The segmentation scheme combines the contextual-clustering and hypothesis-testing schemes because $P(s_k(p)|a_k(p) = 0)$ s, obtained from the SPM $\{s_k\}$, give the probabilities under the null hypothesis of no activation. These probabilities, given \mathbf{a}_k , are obtained by clustering the SPM $\{s_k\}$ into two clusters: activated voxels and inactive voxels. $P(z_k(p)|a_k(p) = 0)$ s are Gaussianly distributed as they are obtained from SPM $\{z_k\}$, and we also assume that $P(z_k(p)|a_k(p) = 1)$ is Gaussian. If a previous segmentation is known, the parameters, namely the mean and the standard deviation, of the distributions can be estimated by using a maximum likelihood criteria [15].

Then the optimal classification can be realized by using a simulated annealing (SA) scheme that maximizes the posterior probability of the configuration [18].

As seen in (9) and (11), a previous segmentation is required to determine the MAP estimation. The local decisions about the activations are iteratively obtained to determine the states of voxels by using an estimation of the activation pattern obtained in the previous iteration; we refer to one *iteration* as a visitation to every voxel site once. After each iteration, the changes of classification, as “flips” in the algorithm, are evaluated repeatedly until convergence or until no changes (or changes less than a small threshold) of classification occurs. Further, the parameters α_{k0} , α_{k1} , β_{k1} , and β_{k2} of the prior model are estimated in each iteration by using a realization of the segmentation [15], [25]. The complete algorithm is given in Algorithm 1. For the segmentation algorithm to begin, a starting activity configuration is obtained by using a noncontextual clustering algorithm—the K -means algorithm [27]—on the SPM. The value of the temperature is initially high and then gradually lowered, in a manner proposed in the SA scheme [14].

Algorithm 1: Segmentation of statistical parameter maps

begin

For all input stimuli k

 Obtain SPM $\{z_k\}$

 Find a segmentation \mathbf{a}_k using the K -means algorithm for two clusters

 Estimate parameters α_{k0} , α_{k1} , β_{k1} , and β_{k2}

 Obtain the parameters of the distributions $P(z_k(p)|a_k(p))$

TABLE I
THE PERCENTAGES OF FALSE NEGATIVES AND FALSE POSITIVES AND THE
TOTAL ERRORS INCURRED IN THE DETECTION OF ACTIVATION IN THE
SYNTHETIC FUNCTIONAL IMAGE AT A S/N RATIO OF -8.5 dB

Percentage of errors	Thresholding of SPM{z}	SPM Approach	MRF Approach
False negatives	2.71	2.71	1.68
False positives	0.88	0.37	0.24
Total errors	3.59	3.08	1.92

```

Fix initial temperature  $T = T_0$  and iteration count  $t = 0$ 
flips = LARGE
Until ( flips > Thresh )
  flips = 0
   $T = T_0/3.0(t + 1)$ 
  For all voxel sites  $p \in \Omega_B$ 
     $a_k^{old}(p) = a_k(p)$ 
    Generate  $a_k^{new}(p)$  randomly
    If  $V(\mathbf{a}_k: a_k(p) = a_k^{old}(p)) > V(\mathbf{a}_k: a_k(p) = a_k^{new}(p))$ 
       $a_k(p) = a_k^{new}(p)$ 
      flips = flips + 1
    Else
      Generate a random number  $\rho \in [0, 1]$ 
      If  $\rho < \exp\{-(V(\mathbf{a}_k: a_k(p) = a_k^{new}(p)) - V(\mathbf{a}_k: a_k(p) = a_k^{old}(p)))/T\}$ 
         $a_k(p) = a_k^{new}(p)$ 
        flips = flips + 1
  Repeat for  $p$ 
  Update parameters  $\alpha_{k0}, \alpha_{k1}, \beta_{k1}$  and  $\beta_{k2}$ 
  Obtain the parameters of the distributions  $P(z_k(p)|a_k(p))$ 
   $t = t + 1$ 
Continue
Repeat for  $k$ 
end

```

IV. EXPERIMENTS AND RESULTS

fMRI has been successfully utilized to localize human brain processes in various sensory or cognitive tasks [20], [28], [29]. The most widely used blood-oxygen-level-dependent contrast fMRI exploits the differences in magnetic susceptibilities of oxygenated hemoglobin and deoxygenated hemoglobin to tract the blood-flow-related phenomena of neuronal activation [28], [30], [31]. During neuronal activation, metabolic rates for oxygen and glucose increase, thus causing changes in local blood flow and oxygenation [32], [33]. The susceptibility changes in blood associated with the concentration of deoxy-hemoglobin create magnetic field inhomogeneities that cause contrast changes in T_2^* weighted magnetic resonance sequences [6], [28], [30], [31], [34], [35]. This enables the fMRI technique to detect hemodynamic changes ensuing neuronal activation.

Here, we present the results of using the present segmentation scheme to detect activation in synthetic functional data, and fMR data obtained in memory retrieval and event-related

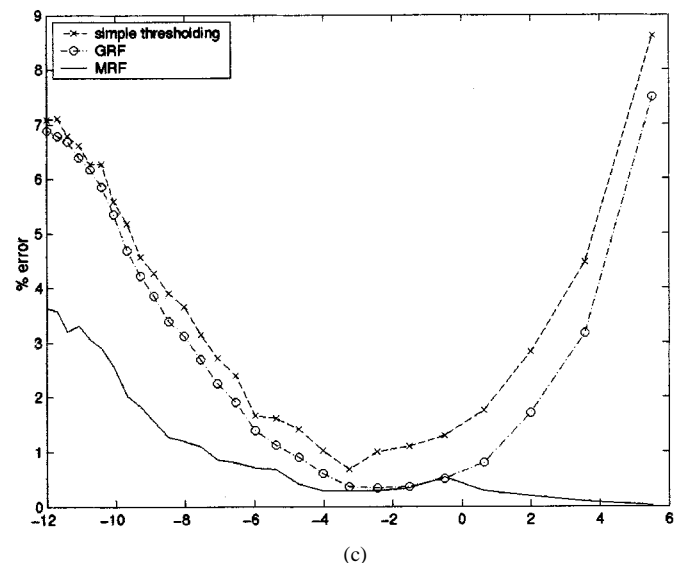
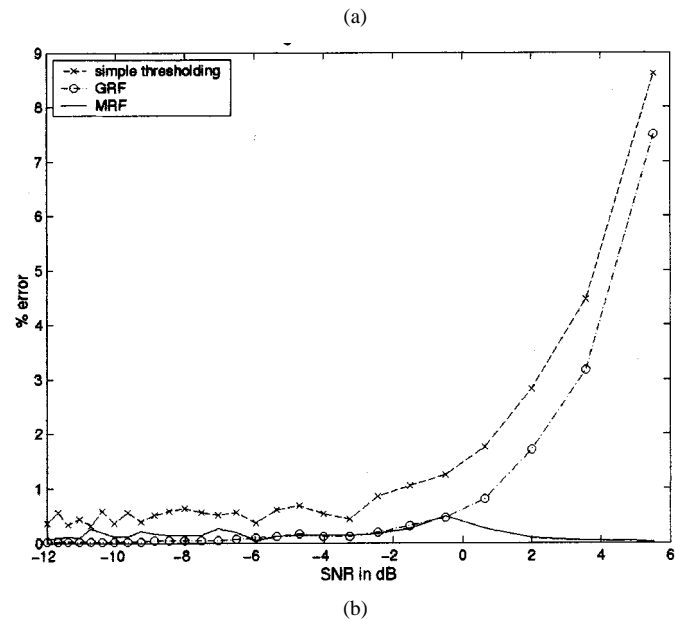
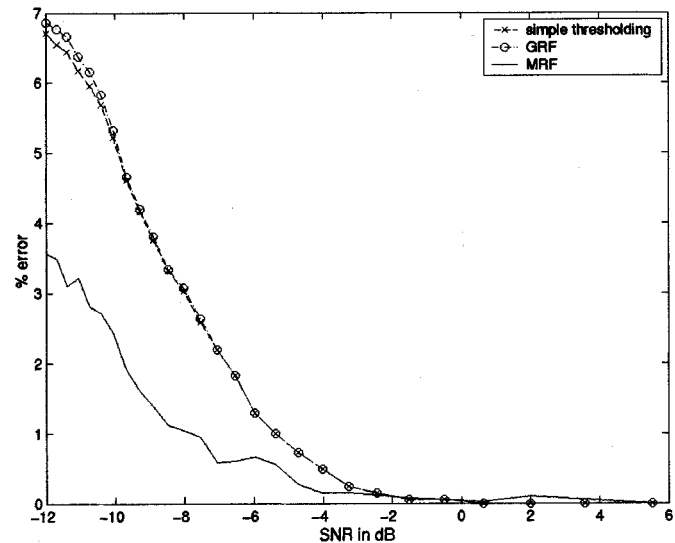


Fig. 4. Illustration of performances of activation detection schemes at various noise levels by the synthetic functional image. Percentages of (a) false negatives, (b) false positives, and (c) the total errors versus the S/N ratio of the image.

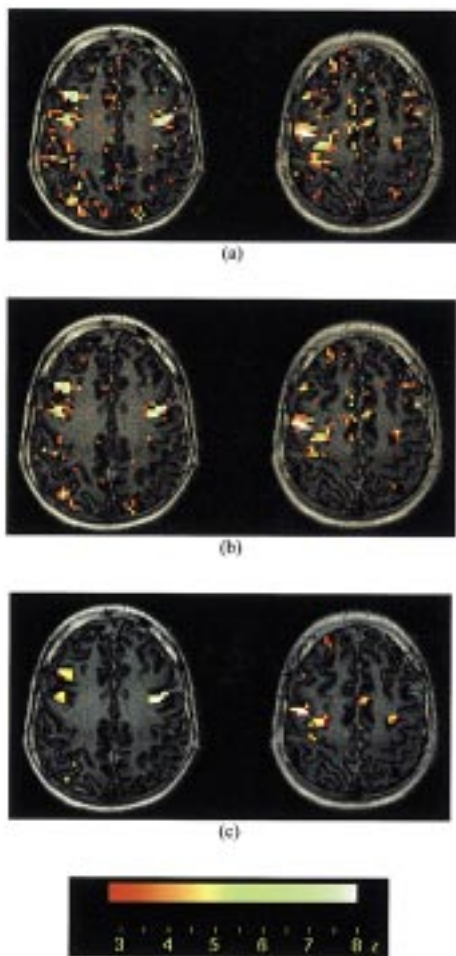


Fig. 5. Activation obtained on two axial brain slices of a representative subject in the memory retrieval task by (a) thresholding the $\text{SPM}\{z\}$ at a significance of $p = 0.01$, (b) using the SPM approach on the $\text{SPM}\{z\}$ with a minimum blob size of three voxels and a significance threshold $z = 3.5$, and (c) using the MRF approach on the $\text{SPM}\{z\}$. The significance values (z -values) of the activated voxels are shown color-coded.

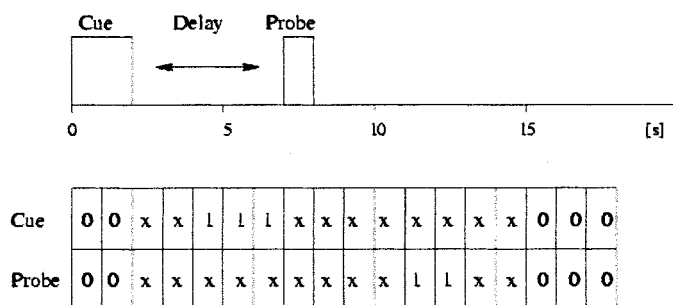


Fig. 6. Illustration of the multistimuli stimulation scheme and the corresponding regressors for the cue and probe phases for the event-related working memory experiment.

working memory tasks. All fMRI images were acquired at the 3T Bruker Medspec 30/100 system at the Max-Planck-Institute of Cognitive Neuroscience, Leipzig, Germany. Prior to the analyses, the images were corrected for baseline variations, by fitting piecewise polynomials [36], and for head motion artifacts, by using the registration package AIR [37], [38]. A significance value or p -value of 0.05 was used for the detection

of the activation with the SPM approach [8] for all fMRI experiments, and after fixing the minimum activation blob size to three, the intensity thresholds for SPMs were adjusted experimentally to obtain the best activation patterns visually. For the simple thresholding approach, the thresholding done at a significance value $p = 0.01$ gave the best activation patterns for all experiments. After the detection of the activation, the significances of activated voxels were color-coded using z statistical values and registered onto the corresponding anatomical scans for display. In all the experiments with the present algorithm, gamma HRF was used, with the empirical values of the parameters set as $\tau_k = 1.25$ and $n_k = 3.0$ [20] for all the stimuli k ; the initial temperature T_0 was set to three; and the threshold of flips (Thresh) was set to zero. The algorithm converged in 80–100 iterations in all experiments.

A. Synthetic Functional Data

A two-dimensional 64×64 synthetic functional image consisting of 64 scans was simulated. Four 9×9 square blobs of pixels were selected to be activated, as shown in Fig. 2(a). The input stimulation was presumed to have eight cycles, each having four stimulation ON states followed by four OFF states, and each stimulation had a duration of 2 s (or $\text{TR} = 2$ s). Box-car time-series were designed for the activated pixels, and the inactive pixels had time-series of zero amplitudes. The responses of the activated pixels were generated by convolving the box-car time-series with a gamma HRF. Gaussian random noise was then added to the time-series of both active and inactive pixels. Pixel intensities of an image scan in the simulated image were given by the values of the time-series at the corresponding time instances. The spatial correlation of the scans was introduced by convolving each functional scan with a Gaussian kernel having FWHM of 3.0, and the images were then properly scaled. If the amplitude of the box-car time-series, represented in the image is h , and the standard deviation of the Gaussian noise is σ , then the signal-to-noise (S/N) power ratio, in dB, is defined as

$$\text{S/N} = 20 \log \left(\frac{h}{\sigma} \right).$$

Fig. 2(b) and (c) shows the sixth and tenth slices, respectively, of the synthetic image at a S/N ratio of -8.5 dB. Fig. 3 shows the detected activation of the synthetic image obtained by a) thresholding the $\text{SPM}\{z\}$ [Fig. 3(a)], using the SPM approach on the $\text{SPM}\{z\}$ with a significance threshold $z = 2.75$ [Fig. 3(b)], and using the MRF approach on the $\text{SPM}\{z\}$ [Fig. 3(c)]. Table I gives the proportions of false positives and false negatives and the total errors rendered by different detection schemes. As seen in the table, the MRF approach had the best overall performance with low values of both false positives and false negatives. Fig. 4 shows the plots of false positives and false negatives and the total errors with different techniques at various S/N levels. Evidently, the MRF approach has better performances at all noise levels—particularly low percentages of false negatives at high noise levels and of false positives at low noise levels. At high signal-to-noise ratio values, the MRF model, because of its spatial correlation model, seems to handle the false positives better than the GRF model in the SPM approach.

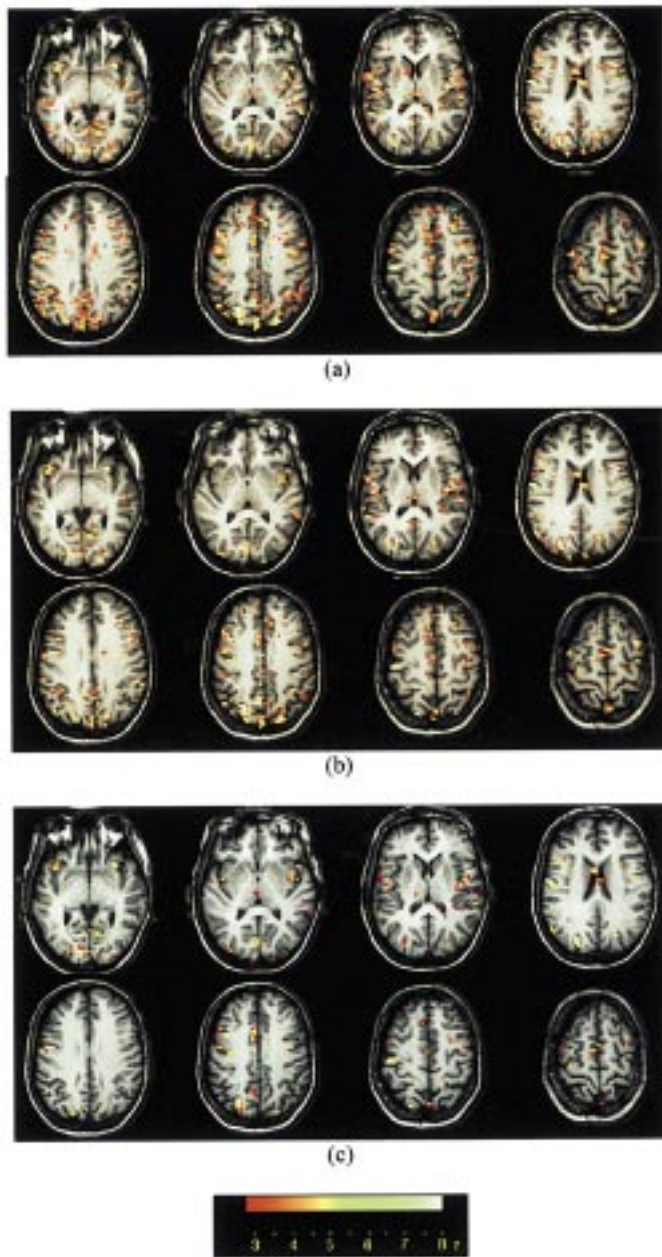


Fig. 7. Activation obtained on eight axial brain slices from a representative subject in the event-related working memory experiment for the cue regressor by (a) thresholding the $SPM\{z\}$ at a significance of $p = 0.01$, (b) using the SPM approach on the $SPM\{z\}$ with a minimum blob size of 3 voxels and a significance threshold $z = 3.0$, and (c) using the MRF approach on the $SPM\{z\}$. The significance values (z -values) of the activated voxels are shown color-coded.

B. Memory Retrieval Task

Prior to the actual experiment, four subjects learned three different sets (sizes 4, 6, and 8) of letters with a corresponding cue for each set. During each trial of the experiment, a cue for the set and a letter were presented, and the subject decided whether the letter corresponded to the indicated set. The processes involved in the brain during the experiment include encoding of the cue and probe, retrieval of information from secondary memory, scanning of primary memory, response selection and response execution. The details of the image acquisition and experiments can be found in [35].

Fig. 5 shows the activation detected on two slices of a representative brain by thresholding the $SPM\{z\}$ [Fig. 5(a)], using the SPM approach on the $SPM\{z\}$ at a significance threshold $z = 3.5$ [Fig. 5(b)], and using the MRF approach on the $SPM\{z\}$ [Fig. 5(c)]. All three methods detected activation in the expected cortical areas; and the activation detected by the MRF based contextual segmentation were focal, local to the cortical areas, and more acceptable and neurophysiologically correct.

C. Event-Related Working Memory Experiment

In this experiment, memory lists comprising of the consonants of the alphabet excluding the letter Y were considered. Subspan sets of sizes 3–6 letters were presented visually for two seconds each (the cue phase), and each was followed by a probe letter (the probe phase) that appeared after a variable delay length (2.0, 3.2, 4.1, 5.2, 6.2, or 7.0 s). Subjects had to decide if the probe letter belonged to a previously presented subspan set. A hit response was given by pressing a button with the ring finger, and the middle finger was used for the foil response. In all, 48 trial combinations [4 (set sizes) \times 6 (delay length) \times 2 (hit/foil manipulation)] were presented randomly in a single run, at an inter-trial interval of 18s, which corresponds to 14.4 min scanning time. There were three experimental runs. Seven subjects took part in the study; two of them completed three runs, while the others completed 4 runs. For further details of the experiment the reader is referred to [39].

Two regressors were constructed for the statistical analysis: the cue regressor and the probe regressor, as shown in Fig. 6. Functional activation was detected by performing multivariate regression with two input stimuli (regressors). Figs. 7 and 8 show the activation obtained on a representative subject for the cue and probe regressors by: 1) thresholding the $SPM\{z\}$; 2) using the SPM approach with the $SPM\{z\}$ at a significance threshold $z = 3.0$; and 3) using the MRF approach. As expected, the left medio-temporal gyrus, the left transverse optical gyrus, and the right posterior parietal cortex showed significant activation with the cue phase, while the left motor cortex was mostly active in the probe phase. The fronto and parietal networks were active in both phases with the MRF approach, as detected with the SPM approach [39]. The activation patterns obtained with the MRF approach were less noisy.

V. CONCLUSION

We have presented a novel method to detect activation from functional brain images. The method accounts for the contextual information of SPMs by assuming that the activation pattern forms an MRF in which the neighborhood interactions and states define the correlation structure. Our experiments support the MRF assumption that mimics both the cooperative interactions of an activated neuron with the activated neighbors and the competition of the neuron with inactive neighboring neurons.

The MRF assumption of the activation pattern gives the prior probabilities to the activity configuration, and therefore the MAP estimation of an activation pattern was derived from likelihoods given by the distributions of SPMs. A scheme based on SA was used to achieve the optimal activity configuration iteratively. The prior model parameters were estimated in

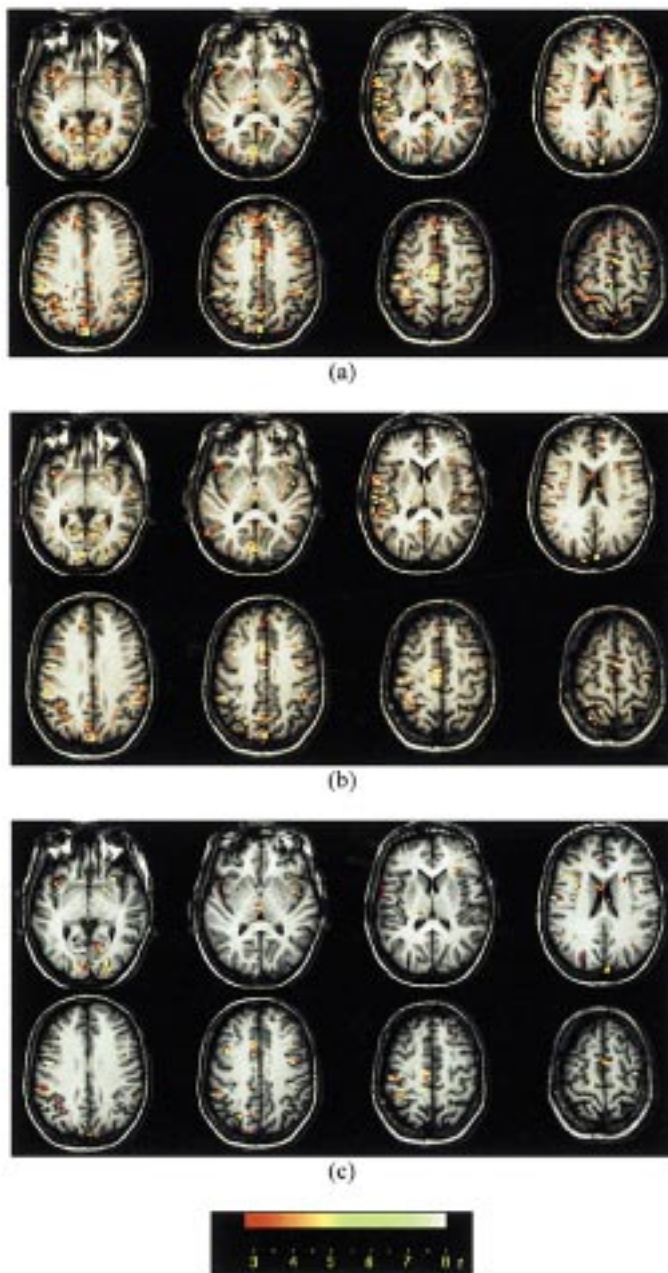


Fig. 8. Activation obtained on eight axial brain slices from a representative subject in the event-related working memory experiment for the probe regressor by (a) thresholding the $SPM\{z\}$ at a significance of $p = 0.01$, (b) using the SPM approach on the $SPM\{z\}$ with a minimum blob size of three voxels and a significance threshold $z = 3.0$, and (c) using the MRF approach on the $SPM\{z\}$. The significance values (z -values) of the activated voxels are shown color-coded.

each iteration by using a segmentation derived in the previous iteration. Our contribution here is the application of a fully data-driven segmentation scheme for testing the voxels for activation, by using both the contextual information and the knowledge of the statistical distribution of the SPM under the null hypothesis. In the experiments, the classical context-free approach produced noisy and unrealistic segmentation of brain activation while the contextual schemes showed more focal realistic brain activation in the cortical regions. In all experiments, the present algorithm converged in near real time;

the longest time taken was 2.3 min for one functional image obtained in the event-related working memory experiment on a Sun UltraSparc 60 350-MHz machine.

In the SPM approach, the corrected significance values for spatial correlations were based on the extents of the activation blobs, and the thresholds were determined empirically to detect significant activation; on the other hand, the MRF approach was free of user-specified parameters, as even the interaction parameters of the prior model were evaluated from an estimation of the segmentation in the previous iteration. That is, our segmentation scheme is fully data-driven, and such an approach gives more accurate results than the approaches (e.g., SPM) that require user-specified parameters. With the MRF approach, more realistic activity patterns, with less noisy and connected blobs of activation, were seen in the experiments. The sensitivities obtained in the MRF approach were higher than those obtained with the thresholding and the SPM approaches; this means that functional experiments can use fewer repetitions and hence have shorter acquisition times.

The proposed technique can be used in experiments involving multiple stimuli, unlike previous similar approaches [1]–[3]. Furthermore, the autocorrelation present in the fMRI time-series was accounted for in the present analysis by considering an HRF. The MRF approach does not require filtering of functional images, and prefiltering in the SPM approach can introduce unnecessary spatial correlation to the SPMs, thereby introducing artifacts in the detected activation patterns. Incidentally, uncorrected baseline variations can introduce artifactual autocorrelations, and motion artifacts introduce spatial correlation to SPMs.

The experiments showed that the knowledge of the correlation model of activation patterns contributed to the reduction of false positives as well as false negatives of activation. Unless the parameters of the correlation models are properly selected, the contextual segmentation schemes may not yield the expected improvements. A comprehensive comparison of the SPM and MRF approaches is not possible because the SPM approach results in a technique with two thresholds, whereas the MRF approach results in an iterative segmentation scheme. Moreover, the unavailability of the gold standards for the activation patterns of the illustrated fMRI experiments did not allow us to determine the superiority in actual experiments of the MRF assumption over the SPM approach. Nevertheless, the experiments with the synthetic data showed better performances with the MRF approach, and, importantly, the MRF approach was fully data-driven.

ACKNOWLEDGMENT

Memory retrieval experiment data were collected while J. C. Rajapakse was a visiting scientist at the Max-Planck-Institute of Cognitive Neuroscience, Leipzig, Germany, and the event-related working memory data was provided by Dr. F. Kruggel. The authors wish to thank V. Venkatraman for helping in the analysis of event-related experiment data, Dr. A. Omondi for proofreading the final manuscript, and the anonymous reviewers for their constructive comments.

REFERENCES

- [1] A. Holmes and I. Ford, "A Bayesian approach to significance testing for statistical images from PET," in *Quantification of Brain Function, Tracer Kinematics in Image Analysis in Brain PET*, K. Uemura et al., Eds. New York: Elsevier Science, 1993.
- [2] X. Descombes, F. Kruggel, and D. Y. von Cramon, "fMRI signal restoration using a spatio-temporal Markov random field preserving transitions," *NeuroImage*, vol. 8, pp. 340–349, 1998.
- [3] —, "Spatio-temporal fMRI analysis using Markov random fields," *IEEE Trans. Med. Imag.*, vol. 17, pp. 1028–1039, Dec. 1998.
- [4] R. S. J. Frackowiak, *Human Brain Function*. San Diego, CA: Academic, 1997.
- [5] R. W. Thatcher, M. Hallett, T. Zeffiro, E. R. John, and M. Huerta, *Functional Neuroimaging: Technical Foundations*. San Diego, CA: Academic, 1994.
- [6] J. C. Rajapakse, F. Kruggel, J. M. Maisog, and D. Y. von Cramon, "Modeling hemodynamic responses for analysis of functional MRI time-series," *Human Brain Map.*, vol. 6, no. 4, pp. 283–300, 1998.
- [7] K. J. Friston, P. Jezzard, and R. Turner, "Analysis of functional MRI time-series," *Human Brain Map.*, vol. 1, pp. 153–171, 1994.
- [8] K. J. Friston, K. J. Worsley, R. S. J. Frackowiak, J. C. Mazziotta, and A. C. Avans, "Assessing the significance of focal activations using their spatial extent," *Human Brain Map.*, vol. 1, pp. 210–220, 1994.
- [9] K. J. Friston, "Statistical parameter mapping," in *Functional Neuroimaging: Technical Foundations*, R. W. Thatcher, M. Hallett, T. Zeffiro, W. R. John, and M. Huerta, Eds. New York: Academic, 1994.
- [10] K. J. Friston, A. P. Holmes, J.-B. Poline, P. J. Grasby, C. R. Williams, R. S. J. Frackowiak, and R. Turner, "Analysis of fMRI time-series revisited," *NeuroImage*, vol. 2, pp. 45–53, 1995.
- [11] E. T. Bullmore, J. Suckling, S. Overmeyer, S. Rabe-Hesketh, E. Taylor, and M. J. Brammer, "Global, voxel and cluster tests, by theory and permutation, for a difference between two groups of structural MR images of the brain," *IEEE Trans. Med. Imag.*, vol. 18, pp. 32–42, Jan 1999.
- [12] J. Besag, "Spatial interaction and the statistical analysis of lattice systems," *J. Roy. Statist. Soc.*, vol. 36, no. B, pp. 192–326, 1974.
- [13] —, "On the statistical analysis of dirty pictures," *J. Roy. Statist. Soc.*, vol. 48, no. 3, pp. 259–302, 1985.
- [14] S. Geman and D. Geman, "Stochastic relaxation, Gibbs distributions, and the Bayesian restoration of images," *IEEE Trans. Pattern Anal. Machine Intell.*, vol. 6, pp. 721–741, June 1994.
- [15] J. C. Rajapakse, J. N. Giedd, and J. Rapoport, "Statistical approach to segmentation of single-channel cerebral MR images," *IEEE Trans. Med. Imag.*, vol. 16, pp. 176–186, Apr. 1997.
- [16] P. A. D. F. R. Hojen-Sorensen, L. K. Hansen, and C. E. Rasmussen, "Bayesian modeling of fMRI time series," *Adv. Neuroinform. Processing Syst.*, vol. 12, pp. 754–760, 2000.
- [17] R. A. Duda, P. A. Hart, and D. G. Stork, *Pattern Classification*, 2nd ed. New York: Wiley, 2000.
- [18] S. Kirkpatrick, C. D. Gelatt, and M. P. Vecchi, "Optimization by simulated annealing," *Science*, vol. 220, no. 4598, pp. 671–680, 1983.
- [19] K. J. Friston, A. P. Holmes, J.-B. Poline, C. D. Frith, and R. S. J. Frackowiak, "Statistical parameter mapping in functional imaging: A general linear approach," *Human Brain Map.*, vol. 2, pp. 189–210, 1995.
- [20] G. M. Boynton, S. A. Engel, G. H. Glover, and D. J. Heeger, "Linear systems analysis of functional magnetic resonance imaging in human V1," *J. Neurosci.*, vol. 16, no. 13, pp. 4207–4221, 1996.
- [21] A. C. Rencher, *Method of Multivariate Analysis*. New York: Wiley, 1995.
- [22] K. J. Friston, C. Frith, P. F. Liddle, and R. S. J. Frackowiak, "The assessment of significant change," *J. Cereb. Blood Flow Metabol.*, vol. 11, pp. 690–699, 1991.
- [23] R. J. Adler, *The Geometry of Random Fields*. New York: Wiley, 1981.
- [24] K. J. Worsley, A. C. Evans, S. Marrett, and P. Neelin, "A three-dimensional statistical analysis for rCBF activation studies in human brain," *J. Cereb. Blood Flow Metabol.*, vol. 12, pp. 900–918, 1992.
- [25] S. Lakshmanan and H. Derin, "Simultaneous parameter estimation and segmentation of Gibbs random fields using simulated annealing," *Appl. Statist.*, vol. 11, no. 8, pp. 799–813, 1989.
- [26] N. Metropolis, A. Rosenbluth, M. Rosenbluth, A. Teller, and E. Teller, "Equations of state calculations by fast computing machines," *J. Chem. Phys.*, vol. 21, pp. 1087–1092, 1953.
- [27] M. R. Anderberg, *Cluster Analysis for Applications*. New York: Academic, 1973.
- [28] P. A. Bandettini, A. Jesmanowicz, E. C. Wong, and J. S. Hyde, "Processing strategies for time-course data sets in functional MRI of human brain," *Magn. Reson. Medicine*, vol. 7, pp. 12–20, 1994.
- [29] K. K. Kwong, J. W. Belliveau, D. A. Chesler, I. E. Goldberg, R. M. Weisskoff, B. P. Poncelet, D. N. Kennedy, B. E. Hoppel, M. S. Cohen, R. Turner, H.-M. Cheng, T. J. Brady, and B. R. Rosen, "Dynamic magnetic resonance imaging of human brain activity during primary sensory stimulation," *Proc. Nat. Acad. Sci, USA*, vol. 89, pp. 5675–5679, 1992.
- [30] R. S. Menon, S. Ogawa, D. W. Tank, and K. Ugurbil, "The gradient recalled echo characteristics of photic stimulation-induced signal changes in the human primary visual cortex," *Magn. Reson. Med.*, vol. 30, pp. 380–386, 1993.
- [31] S. Ogawa, R. S. Menon, D. W. Tank, S.-G. Kim, H. Merkle, J. M. Ellermann, and K. Ugurbil, "Functional brain mapping by blood oxygenation level dependent contrast magnetic resonance imaging," *Biophys. J.*, vol. 64, pp. 803–812, 1993.
- [32] A. Villringer and U. Dirnagl, "Coupling of brain activity and cerebral blood flow: Basis of functional neuroimaging, cerebrovascular and brain metabolism review," *Cerebrovasc. Brain Metabol. Rev.*, vol. 7, pp. 240–276, 1995.
- [33] M. Jueptner and C. Weiller, "Review: Does measurement of regional cerebral blood flow reflect synaptic activity?—Implications for PET and fMRI," *NeuroImage*, vol. 2, pp. 148–156, 1995.
- [34] R. B. Buxton and L. R. Frank, "A model for the coupling between cerebral blood flow and oxygen metabolism," *J. Cereb. Blood Flow Metabol.*, vol. 17, pp. 64–72, 1997.
- [35] J. C. Rajapakse, F. Kruggel, S. Zysset, and D. Y. von Cramon, "Neuronal and hemodynamic events from fMRI time-series," *J. Adv. Computational Intell.*, vol. 2, no. 6, pp. 185–194, 1998.
- [36] V. Venkatraman, J. C. Rajapakse, and S. S. Abeysekara, "Baseline correction of functional MR time-series," in *Proc. Int Conf. Neural Information Processing (ICONIP2000)*, Taejeon, Korea.
- [37] R. P. Woods, S. R. Cherry, and J. C. Mazziotta, "Rapid automated algorithm for aligning and reslicing PET images," *J. Comput. Assist. Tomogr.*, vol. 16, pp. 620–633, 1992.
- [38] —, "MRI-PET registration with automated algorithm," *J. Comput. Assist. Tomogr.*, vol. 17, pp. 536–546, 1993.
- [39] F. Kruggel, S. Zysset, and D. Y. von Cramon, "Nonlinear regression of functional MRI data: An item recognition study," *NeuroImage*, vol. 12, pp. 173–183, 2000.



Jagath C. Rajapakse (S'90–M'91–SM'00) received the B.Sc. (Eng.) degree with First Class Honors from University of Moratuwa, Sri Lanka, in 1985, and won the award for the best undergraduate in electronic and telecommunication engineering. He received the M.Sc. and Ph.D. degrees in electrical and computer engineering from the State University of New York, Buffalo, in 1989, and 1993, respectively.

He was a Visiting Fellow with the National Institute of Mental Health, Bethesda, MD, from 1993–1996, and a Visiting Scientist at the Max-Planck-Institute of Cognitive Neuroscience, Leipzig, Germany. In May 1998, he joined Nanyang Technological University, Singapore, where he is presently an Associate Professor in the School of Computer Engineering. His current research interests are in neural networks, medical imaging and bioinformatics. He is author or co-author for more than 85 publications. <http://www.ntu.edu.sg/home/asjagath/home.htm>

Dr. Rajapakse is a recipient of the Fulbright Scholarship.



Jayasanka Piyaratna (S'00–M'01) received the B.E. (electrical and electronic) degree with First Class Honors from The University of Adelaide, Adelaide, Australia, in 1999 after having been awarded an AUSAID Scholarship. He recently received the M.Eng. degree in computer engineering from Nanyang Technological University, Singapore, after having been awarded a second scholarship.

In March 2001, he joined DSpace Pty. Ltd., Adelaide, Australia, where he is currently a Software Systems Engineer. He is author or co-author of more than

ten publications.